

# Satellite snow-cover monitoring for the prediction of snowmelt runoff in the upper reaches of the Yellow River, China

ZENG QUNZHU, FENG XUEZHI, CHEN XIANZHANG, LAN YONGCHAO, WANG JIAN  
*Lanzhou Institute of Glaciology and Geocryology, Academia Sinica, Lanzhou 730000, China*

AND LIU YUJIE  
*Satellite Meteorology Centre, State Meteorological Administration, Beijing 10081, China*

**ABSTRACT.** Spatial-temporal variations in the extent of the seasonal snow cover of the upper reaches of the Yellow River were studied systematically, using NOAA, Landsat, MSS and TM images, supported by ground-truth data. Effects of changing areal extent of snow cover on river flow were also examined. Spring-runoff forecasting models were developed, based on ridge regression methods and Grey theory, employing satellite snow-cover and actual hydrometeorological data to forecast inflow to the Longyang Gorge reservoir for ten-day periods between April and early June. Forecast precision is within  $\pm 15\%$  of the actual observation. Separating snow-cover data by elevation zone improves the accuracy of forecast over lumping snow cover over the entire basin.

## GENERAL SITUATION OF THE BASIN AND THE RESEARCH CONTEXT

### General situation of the basin

The upper reaches of the Yellow River are situated in the northeast of the Qinghai-Xizang Plateau (Figure 1). The mean elevation of the basin is over 3200 m and Maqengangrti (the highest peak) rises to 6282 m a.s.l. The study basin extends from the source of the Yellow River to Tangnag Hydrometric Station with long axis of 1172 km and area of 121,972 km<sup>2</sup>. Because of relatively abundant precipitation, in the range of 300 to 750 mm a<sup>-1</sup>, low annual mean temperature between -4.0 to 1.1 °C, and little evaporation, specific runoff reaches 6.5 dm<sup>3</sup> s<sup>-1</sup> km<sup>-2</sup> in this area, which is about three times as high as the mean value of the entire Yellow River basin. Throughout the Yellow River basin, snow and glaciers are widely distributed, with 57 glaciers around Maqengangrti peak area of 120.57 km<sup>2</sup>. Meltwater from glaciers and snow is one of the main supply sources of spring runoff in the upper reaches of the Yellow River, accounting for about 70% of surface runoff between late March and mid-June.

### The research context

The continuous monitoring of winter-spring snow cover in the area and the operational forecasting of spring runoff have been carried out using the Ice, Snow and Water Resources Information System (ISWRIS), which is a spatial data system with snow-cover information

extracted from NOAA-9, -10 and -11, AVHRR, Landsat Thematic Mapper (TM), MSS imagery or CCT data, actual hydrometeorological data, and field investigations. The aim of the research is to provide a scientific basis for the operation and management of the Longyang Gorge reservoirs in the upper reaches of the Yellow River.

## SATELLITE SNOW-COVER MONITORING AND SNOW DISTRIBUTION IN THE BASIN

### Information correction and data processing

#### (a) NOAA AVHRR data

Real-time NOAA AVHRR positive transparencies from channel I to channel IV with longitude-latitude grid are processed using a NAC-4200F Multicolour Data System as follows: first, a basin boundary is established over the 1:1 000 000 topographic map, and the river watershed added; channel IV (10.2 to 11.3  $\mu\text{m}$ ) and channel I (0.58 to 0.68  $\mu\text{m}$ ) images are set up successively on the screen when the images of channel I and channel II have been matched and superimposed. Second, in the procedure of density slicing, a contrast stretch is applied. Adjustment of pixel brightness is undertaken visually so that the proper brightness range of snow cover can be determined on the image. The snow-covered area is then extracted by density slicing and the graded colouring of snow-covered area. Calculation of snow-cover percentage is as follows:

$$R = S_f / B_f \quad (1)$$

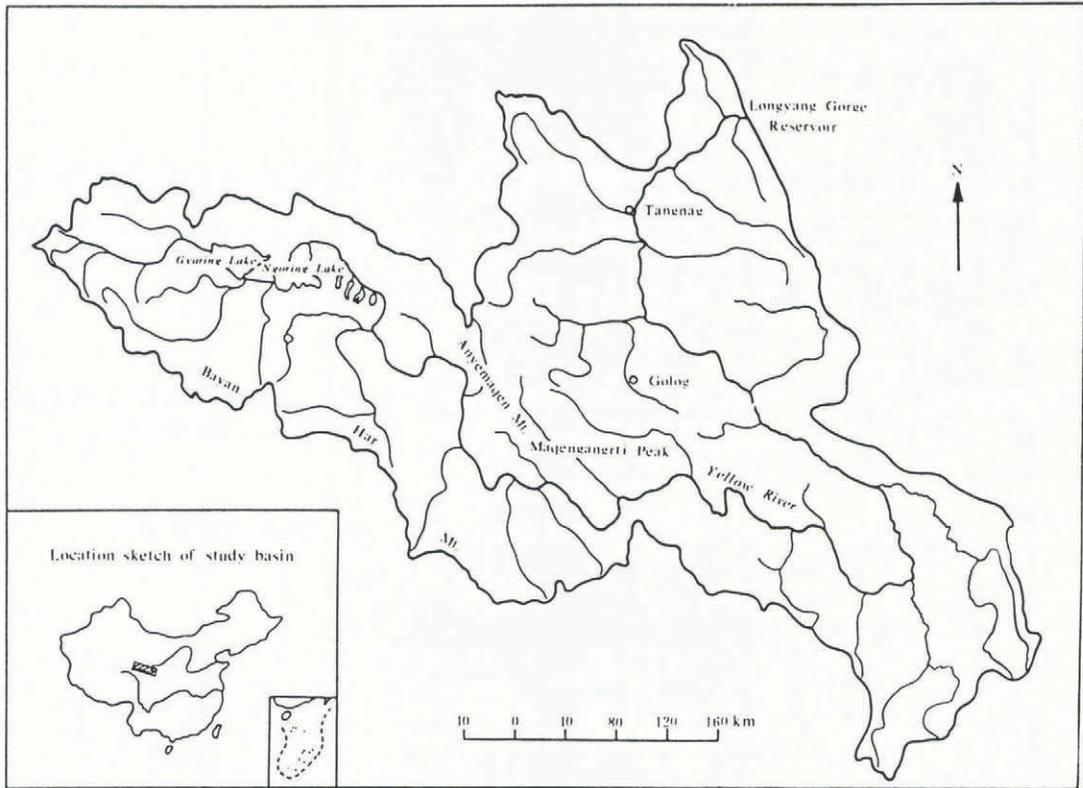


Fig. 1. Map of the basin of the upper reaches of the Yellow River above Tangnaihai Hydrometric Station.

where  $R$  is the snow-cover percentage of the basin;  $S_f$  is the snow-cover percentage within a rectangular range, and  $B_f$  is the areal percentage of the basin relative to the rectangular range.

(b) AVHRR/HRPT digital data

The preprocessing of the AVHRR/HRPT (High Resolution Picture Transmission, with about  $1\text{ km}^2$  spatial resolution) data is carried out as follows: the CCT “1B” data set is created after correction of solar zenith angles and limb darkening; then a stereographic mosaic of AVHRR data from three orbits is used so that image distortion can be minimized. The cloud effect can also be eliminated, by use of the “7-day minimum brightness” method according to the difference in brightness between cloud and snow and how the shape and area of cover vary with time on the image (Liu, 1987).

The image data file can be created through the formula below:

$$G(I, J) = \min\{g_1(I, J), g_2(I, J) \dots g_7(I, J)\} \quad (2)$$

where  $G(I, J)$  is the minimum brightness in 7 days at the point  $(I, J)$  and  $g_i(I, J)$  is the minimum brightness on a certain day ( $i$ ) at the point  $(I, J)$ .

The calibrated reflectance of NOAA AVHRR in the visible channel can be calculated as follows:

$$R_k = S_i G + I_i \quad (3)$$

where  $R_k$  is the reflectance of the ground surface after the correction of solar zenith angles;  $G$  is the brightness of any point on the composite image, and  $S_i$  and  $I_i$  are the calibration coefficients of the visible channel.

Nine levels of brightness were separated by density

slicing. The reflectance interval is 10% from level 0 to level 8, and level 9 is defined as the pixels outside the basin. Levels 0 and 1, and levels 2 and 3 represent the background and snow respectively, based on the logic analysis of season and the characteristics of the ground object. Tests show that it is reasonable that the snow data of the basin are extracted using the above interpretation criteria. The snow cover interpreted is put into the forecast model of snowmelt runoff as a variable.

(c) AVHRR/APT images

For the AVHRR/APT (Automatic Picture Transmission with resolution  $4\text{ km}^2$ ) images with large distortion (provided by provincial meteorological observatories), after geometric correction, snow-covered areas are transferred from the image onto the topographic map and then measured.

(d) Snow-cover charts

A series of charts of snow cover at the scale 1 : 1 500 000 is mapped, based on AVHRR, APT images and field data on snow depth and the characteristics of snow distribution of the basin.

According to analysis of NOAA APT and AVHRR images for the fifteen years (1976–90), stable seasonal snow cover begins at the end of September or the beginning of October; the snow-covered area extends gradually from higher to lower elevations and from south to north, reaching maximum extent in the first ten days of April of the following year. Then, the area begins to contract day by day. The seasonal snow cover melts away by the first ten days of June, except in the firm basin of Anyemaqen mountain. Table 1 gives the mean value of

Table 1. The mean snow-covered area in the study area for each ten-day period between 20 March and 30 May for the years 1976 to 1990

	March		April		May		
snow area snow cover (%)	III	I	II	III	I	II	III
	9.8	10.3	7.6	7.4	5.0	7.1	3.7
snow area (km <sup>2</sup> )	11 953	12 562	9269	9025	6098	8659	4512

snow-cover percentage in the study area over the years from 1976 to 1990, from the last ten days of March to the last ten days of May on the basis of APT and AVHRR data.

## MAIN FACTORS INFLUENCING SPRING RUN-OFF

### (a) Relationships between snow-cover percentage and spring runoff

Analysis of AVHRR images since 1982 shows that there was abundant snow in the upper reaches of the Yellow River for the years 1982, 1983, 1989 and 1990 with correspondingly larger spring-runoff amounts. Figure 2 shows the close relationship between percentage snow cover in the basin in the last ten days of April and the mean discharge at Tangnag in the first ten days of May.

### (b) Spring precipitation and air-temperature effects on runoff

Rainfall in the spring had little effect on runoff. The correlation coefficient between liquid precipitation and runoff in each month between March and June was only 0.02, 0.10, 0.31 and 0.51, respectively, for each month. Although solar radiation is the most important heat source, followed by sensible heat, air temperature can strongly influence the pattern of spring runoff.

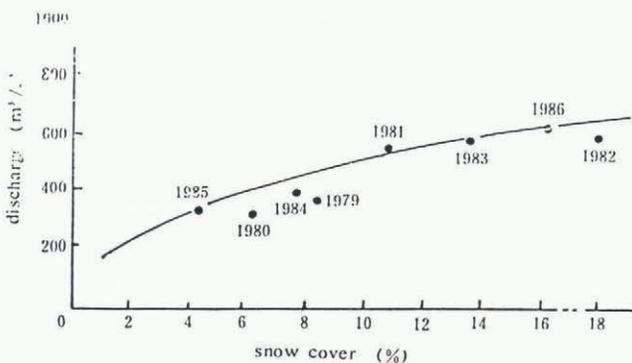


Fig. 2. Relationship between mean discharge of the first ten days of May over the years 1979–86 at the Tangnag Hydrometric Station and the snow-cover percentage in the last ten days of April in the Anyemagen mountains.

## SIMULATION AND FORECASTING OF SPRING RUNOFF

### (a) Selection of reference stations and forecasting factors

In forecasting each ten-day inflow,  $Y$ , to Longyang Gorge reservoir from the first ten days of April to the first ten days of June, principal components analysis and cognate analysis (Luo and Xin, 1987) were used to select reference stations and forecasting factors. The following variables are used:  $X_1$ : the mean snow-cover percentage (MSCP) of the study area in October of last year (the higher the percentage of snow cover the more snow remains to contribute to spring runoff);  $X_2$ : the MSCP in the ten days before issuing a forecast;  $X_3$ : the mean discharge ( $m^3 s^{-1}$ ) at Tangnag Hydrometric Station in the ten-day period before issuing a forecast;  $X_4$ : the mean maximum temperature ( $^{\circ}C$ ) in October of last year at the Gulog Meteorological Observatory (GMO);  $X_5$ : precipitation (mm) in October of last year at GMO;  $X_6$ : the mean maximum temperature ( $^{\circ}C$ ) at GMO in the ten days before issuing a forecast;  $X_7$ : the precipitation (mm) ten days before issuing a forecast at GMO. The results of the cognate analysis are listed in Table 2.

According to the needs of the Longyang Gorge reservoir, models were developed to forecast spring runoff in the upper reaches of the Yellow River using snow information from NOAA, and actual hydrometeorological data by the use of mathematical statistics, Grey system theory (Deng, 1986) and ridge regression analysis (Luo and Xin, 1987). The following formula is used for calculating the ridge regression coefficient,  $B(K \geq 0)$ :

$$\hat{B}(K_0) = (X'X + K_0I)^{-1}X'Y \quad (4)$$

where  $I$  is the unit matrix,  $K_0$  is the ridge parameter;  $\hat{B}(K_0)$  is the estimated value of ridge regression coefficient. When  $K = 0$ , the formula above is the Ordinary Least Square Estimation (OLSE),  $B(K_0)$  can be calculated by the following formula:

$$B_i(K_0) = \frac{\left[ \sum_{j=0}^p \{S_{0j}S_{ij}/(\lambda_j + K_0)\} \right]}{\left[ \sum_{j=0}^p \{S_{0j}^2/(\lambda_j + K_0)\} \right]} \quad (5)$$

Table 2. Results of cognate degree analysis between forecasted variable and predictor variables

Factor	Forecasted	Predictor variables						
	$Y$	$X_1$	$X_2$	$X_3$	$X_4$	$X_5$	$X_6$	$X_7$
cognate degree	1	0.69	0.78	0.87	0.57	0.62	0.46	0.67
cognate order		3	2	1	6	5	7	4

where  $i = 1, 2, \dots, p$ ;  $p$  is the number of the predictors;  $\lambda_j$  and  $S_{ij}$  are the characteristic value and eigenvector of  $X'X$  augmented matrix, respectively. The forecast value is

$$Y = XB(K_0) + \varepsilon \tag{6}$$

where  $X$  is the predictor;  $B(K_0)$  is the ridge regression coefficient; and  $\varepsilon$  is the residual.

The ridge regression method was used for forecasting the inflow to the Longyang Gorge reservoir over ten-day periods from April to the first ten days of June. Comparisons of predicted runoff with actual measured data in 1989 and 1990 show that the forecast precision is within the permitted error range specified by the reservoir managers (within 20% of measured values).

**(c) Simulation of spring runoff**

Under the support of ISWRIS, the Qushman River basin, a first-order stream with its source in Anyemaqen mountain in a representative area of the upper reaches of the Yellow River, was divided into three elevation zones: zone A (below 3900 m a.s.l.), zone B (3900 to 4650 m a.s.l.) and zone C (above 4650 m a.s.l.). The snow-cover percentage in each zone was obtained from AVHRR data. The following models were established to calculate the mean discharge of the Qushman River in the period from the last ten days of March to the first ten days of June and in April:

$$Q_t = (1 - k)(-143.39 + 0.345P_A + 1.214S_A + 0.3P_B + 0.72S_B + 0.58S_C - 12.98T_C) \tag{7}$$

where  $Q_t$  is daily mean discharge ( $m^3 s^{-1}$ ) from the last ten days of March to the first ten days of June at Damitan Hydrometric Station on the Qushman River;  $k$  is the recession coefficient of discharge;  $P_A$  is the precipitation (mm) at Golog Meteorological Station;  $S_A$  is the snow-cover percentage (SCP) in zone A;  $P_B$  is the precipitation (mm) at Renxiamu Meteorological Station;  $S_B$  is the SCP in zone B;  $S_C$  is the SCP in zone C and  $T_C$  is the air

temperature ( $^{\circ}C$ ) at Golmud Meteorological Station, all variables for the same time period.

$$Q_{IV} = (1 - k)(48.57 - 0.47S_A + 0.3P_A - 0.31S_B - 0.2T_B - 0.213S_C) \tag{8}$$

where  $Q_{IV}$  is the daily mean discharge ( $m^3 s^{-1}$ ) in April (same period for following parameters) at Damitan Hydrometric Station;  $k$  is the recession coefficient (actual value: 0.2) of discharge;  $T_B$  is the daily mean temperature ( $^{\circ}C$ ) at Renxiamu Meteorological Station, and the other symbols are as in Equation (7).

Table 3 shows a comparison between calculated value and measured data for the two models using the snow data separated into the three elevation zones and lumped for the entire basin. Accuracy of forecast is considerably improved by separation of snow-cover data into three elevations zones rather than by using snow cover for the entire basin.

**ACKNOWLEDGEMENTS**

The other persons who attended some of the field expeditions and indoor data analyses are Li Wenzhong, Zhang Shunxing, Tang Han, Liang Fengxian, Wang Guangyu, Liu Jinghuang, Pu Yibin and others. The Satellite Meteorology Centre, State Meteorological Administration, the Environment Forecasting Centre of National Oceanic Administration of China, the Meteorological Bureaus of Gansu and Qinghai Provinces provided meteorological data and other relative data. The Longyang Gorge water power plant gave assistance with testing and verifying of spring-runoff forecast. The assistance of the above is gratefully acknowledged.

**REFERENCES**

Deng Julong. 1986. *Grey forecast and decision*. Wuhan, Press

Table 3. Actual discharges of the Qushman River, and predicted values obtained using snow-cover data zoned by elevation band or snow-cover data for the entire basin

Year	Period	Measured data	Calculated value (zoned)	Calculated value (entire basin)	Error(%)	
		$m^3 s^{-1}$	$m^3 s^{-1}$	$m^3 s^{-1}$	zoned	entire basin
1988	20 March to 10 June	20.6	20.3	16.5	-1.4	-19.7
1989	20 March to 10 June	31.7	30.9	23.4	-2.4	-26.0
1988	April	13.9	11.2	9.7	+19.2	-30.6
1989	April	11.6	10.8	13.8	-7.1	+18.9

- of Huazhong College of Engineering.
- Hall, D. K. and J. Martinec. 1985. *Remote sensing of ice and snow*. London, etc., Chapman and Hall.
- Liu Yujie. 1987. *Ice and snow cover monitoring using satellite data*. Beijing, State Meteorological Administration. Satellite Meteorology Centre.
- Luo Jiyu and Xin Yin. 1987. *Statistical and analytical method on economics and forecast*. Beijing, Press of Qinghua University.
- Rango, A. and J. Martinec. 1979. Application of a

snowmelt-runoff model using Landsat data. *Nord. Hydrol.*, **10**(4), 225–238.

- Zeng Qunzhi, Zhang Shunying, Chen Xianzhang and Wang Jian. 1987. Satellite snow-cover monitoring in the Qilian mountains and an analysis for characteristics of stream snow-melt run-off in the Hexi region, Gansu, China. *Ann. Glaciol.*, **9**, 225–228.

*The accuracy of references in the text and in this list is the responsibility of the author/s, to whom queries should be addressed.*